THE ASTROPHYSICAL JOURNAL, 495:927–932, 1998 March 10
© 1998. The American Astronomical Society. All rights reserved. Printed in U.S.A.

LARGE VARIATIONS IN THE WINDS OF SINGLE COOL GIANTS: λ VELORUM AND γ CRUCIS[1]

D. J. MULLAN[2]
Bartol Research Institute, University of Delaware, Newark, DE 19716
K. G. CARPENTER
NASA Goddard Space Flight Center, Laboratory for Astronomy and Solar Physics, Code 681, Greenbelt, MD 20771
AND
R. D. ROBINSON
NASA Goddard Space Flight Center, Astronomy Programs, Computer Sciences Corporation, Code 681/CSC, Greenbelt, MD 20771
Received 1997 August 11; accepted 1997 October 20

ABSTRACT

UV spectra of the "noncoronal" single K supergiant λ Vel and of the single M giant γ Cru obtained with *IUE* and the *Hubble Space Telescope* at various epochs indicate that the profiles of many lines formed in the wind exhibit striking alterations in shape with time. We parameterize the wind profiles in terms of an empirical optical depth $\tau_{\rm emp}$ by reflecting the red wing about line center and comparing the reflected intensity with that of the blue wing. In the λ Vel wind the terminal velocity v_∞ was found to be close to 40 km s^{-1} in 1978, 1982, and 1994, but was at least 20 km s^{-1} greater in 1990. The faster wind in 1990 also had a total optical depth that was a factor of 2–6 times greater than at the other epochs.

Subject headings: line: profiles — stars: mass loss — stars: late-type — ultraviolet: stars

1. INTRODUCTION

Stars in the upper right-hand corner of the H-R diagram are classified as "coronal," "noncoronal," or "hybrid," depending on the presence or absence of hot material in the atmosphere and on the properties of the wind (Hartmann et al. 1980; Ayres et al. 1981). "Noncoronal" cool giants lose mass in the form of slow winds, as the terminal velocity v_∞ is typically small compared to the photospheric escape speed $v_{\rm esc}$.

Several mechanisms have been proposed to explain the driving of "noncoronal" winds. Radiation pressure on dust grains may be relevant in MIa stars. For warmer stars or for stars with higher gravity, various magnetic mechanisms might be at work. Thus, Alfvén waves provide quantitative models of steady wind driving in "hybrid" stars (Brosius & Mullan 1986). Alfvén waves possibly also drive mass loss in "noncoronal" stars, although it is difficult to have $v_\infty \ll v_{\rm esc}$ unless the Alfvén wave dissipation length is fine-tuned to have a value almost exactly equal to 1 stellar radius (Leer et al. 1982). A second class of magnetic driving is intrinsically variable: discrete magnetic structures can be ejected from time to time when magnetic equilibrium in an active region is lost. In the solar wind, on the largest scales, this variable component is detectable in the form of coronal mass ejections (CMEs), which contribute at least 16% to the solar mass loss rate at maximum activity (Jackson & Howard 1993).

In this paper we discuss wind diagnostics for two isolated (i.e., nonbinary) "noncoronal" stars, the K5 Ib-II supergiant λ Vel and the M3.4 III giant γ Cru. We found large variations of the winds in both stars on timescales of a few yr. We concentrate our analysis here on the variations in λ Vel.

2. OBSERVATIONS AND DATA ANALYSIS

Both λ Vel and γ Cru were observed by *IUE* at high resolution a number of times during the lifetime of the spacecraft. Table 1 lists the images we have used.

All *IUE* spectra were reduced using the IUEHI procedure in IUERDAF to convert the net flux numbers to absolute fluxes in ergs cm^{-2} s^{-1} Å^{-1}. The wavelength scale was converted to velocity by using the laboratory wavelength shifted to the rest frame of the star (radial velocity = +18 km s^{-1} for λ Vel and +21 km s^{-1} for γ Cru). *IUE* exposures prior to 1980 appear to have systematic wavelength shifts of 10–30 km s^{-1}. We have removed this offset under the assumption that it is a zero-point error in the wavelength scale, typical of early *IUE* images.

Spectra of λ Vel were also obtained with the Goddard High Resolution Spectrograph (GHRS) aboard the *Hubble Space Telescope* on 1994 September 3–4 (GO program 5307). The data for the present analysis consist of medium-resolution (G270M) spectra of a set of mid-UV Fe II lines having a range of intrinsic line strengths. Dedicated wavelength calibration exposures on the on-board platinum lamps (referred to as WAVECALS) were obtained close in time to each of the stellar observations. These, combined with the fact that the star was observed through the 0.″22 square small science aperture, allow us to determine the dispersion coefficients and absolute wavelengths to an accuracy of about 3 km s^{-1} in G270M. The observations were calibrated with the CALHRS routine developed by the GHRS Investigation Definition Team (IDT). This routine eliminates or reduces the effects of weak diodes, subtracts background and scattered light, corrects for vignetting and echelle ripple, and applies absolute calibrations to fluxes and wavelengths.

3. RESULTS: SPECTRAL LINE VARIABILITY

The profiles of four Fe II lines in the UV spectrum of λ Vel are shown in Figure 1 for two epochs. Two of the lines

[1] Based on observations with the NASA/ESA *Hubble Space Telescope*, which is operated by the Association of Universities for Research in Astronomy, Inc., under NASA contract NAS 5-26555, and on observations with the *International Ultraviolet Explorer*.

[2] NASA/ASEE Summer Faculty Fellow, NASA Goddard Space Flight Center, Laboratory for Astronomy and Solar Physics, Greenbelt, MD 20771.

TABLE 1

IUE IMAGES FOR PROGRAM STARS

Star	*IUE* Number	Year	Exposure (minutes)
λ Vel	LWR 03208	1978	20
λ Vel	LWR 13536	1982	270
λ Vel	LWP 08332	1986	100
λ Vel	LWP 19277	1990	420
γ Cru.....	LWR 01356	1978	72
γ Cru.....	LWP 08472	1986	60

belong to UV multiplet 1 (λ2585.876 Å lower excitation potential $\chi_{lo} = 0.0$ eV; λ2621.669 Å $\chi_{lo} = 0.12$ eV), one to UV multiplet 63 (λ2739.548 Å $\chi_{lo} = 0.98$ eV), and one to UV multiplet 64 (λ2591.543 Å $\chi_{lo} = 1.04$ eV). The relative strengths of these lines can be estimated by comparison with a relative optical depth scale τ_0 that will be defined below: the four lines in Figure 1 have τ_0 values that span a range of about 20. However, despite this range in line strength, all four lines show similar behavior. Thus, the emission peak and wing on the *red* side of all four lines are reproducible between the two exposures (allowing for some saturation effects in certain pixels in the *IUE* images). On the other hand, there are striking differences between the profiles on the *blue* side of the line (where no saturation is present in the *IUE* data): a prominent blue peak occurs in 1994 in all four lines, but this blue peak is essentially absent in 1990.

The striking changes in profile between 1990 and 1994 are also apparent in other Fe II lines, as well as in lines of other species and other degrees of ionization (Mg I, Mn II). Thus, the alterations shown in Figure 1 between 1990 and 1994 do not simply result from a change in the ionization state of iron, and we conclude that the column density of the wind must have changed.

To illustrate that the wind variations observed in λ Vel are not unique among cool giants, in Figure 2 we show the profiles of four Fe II lines in γ Cru taken at two epochs (1978 and 1986) by *IUE*. Three of the lines are the same as those in Figure 1; however, in order to broaden the wavelength range of our comparison (because of possible differences between LWP and LWR cameras; see below), we replace one line in Figure 1 with another at a much shorter wavelength, λ2332.800 Å ($\chi_{lo} = 0.05$ eV). Although the noise level is rather high in the *IUE* spectra, the alterations from one epoch to the other are unmistakable, and they strongly resemble those seen in λ Vel. We note that the spectrum obtained in 1978 was obtained with the LWR camera, while in 1986, the LWP camera was used. The fact that the two images of γ Cru were taken with different cameras is not of great consequence in the present context for the following reasons. It is true that in the wavelength range of interest, the signal-to-noise ratio of a high-resolution image in the

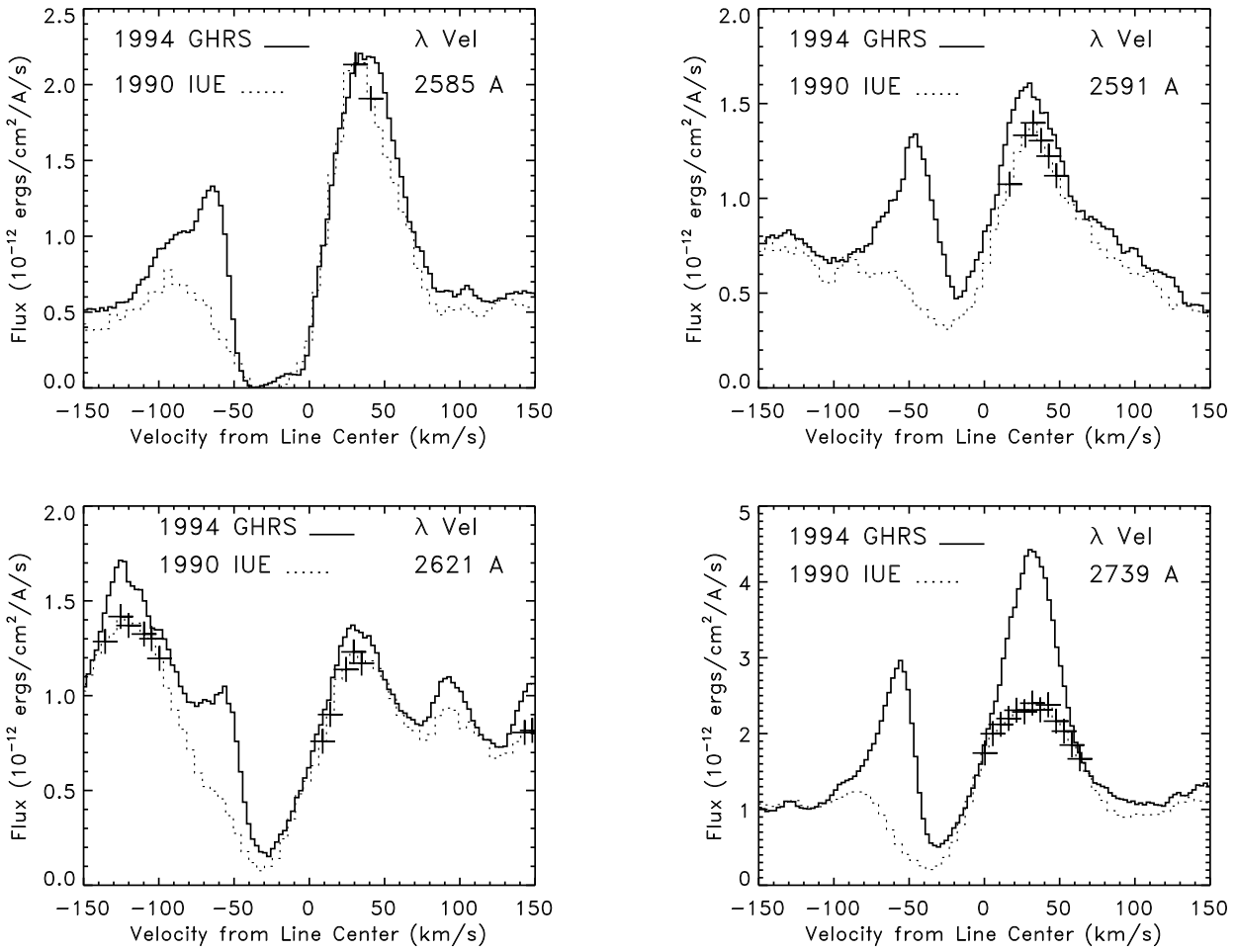


FIG. 1.—Comparison of profiles of four Fe II lines at two epochs in λ Vel. Crosses indicate points of poor quality in *IUE* data (i.e., those affected by saturation of detector pixels or reseau marks on the detector faceplate).

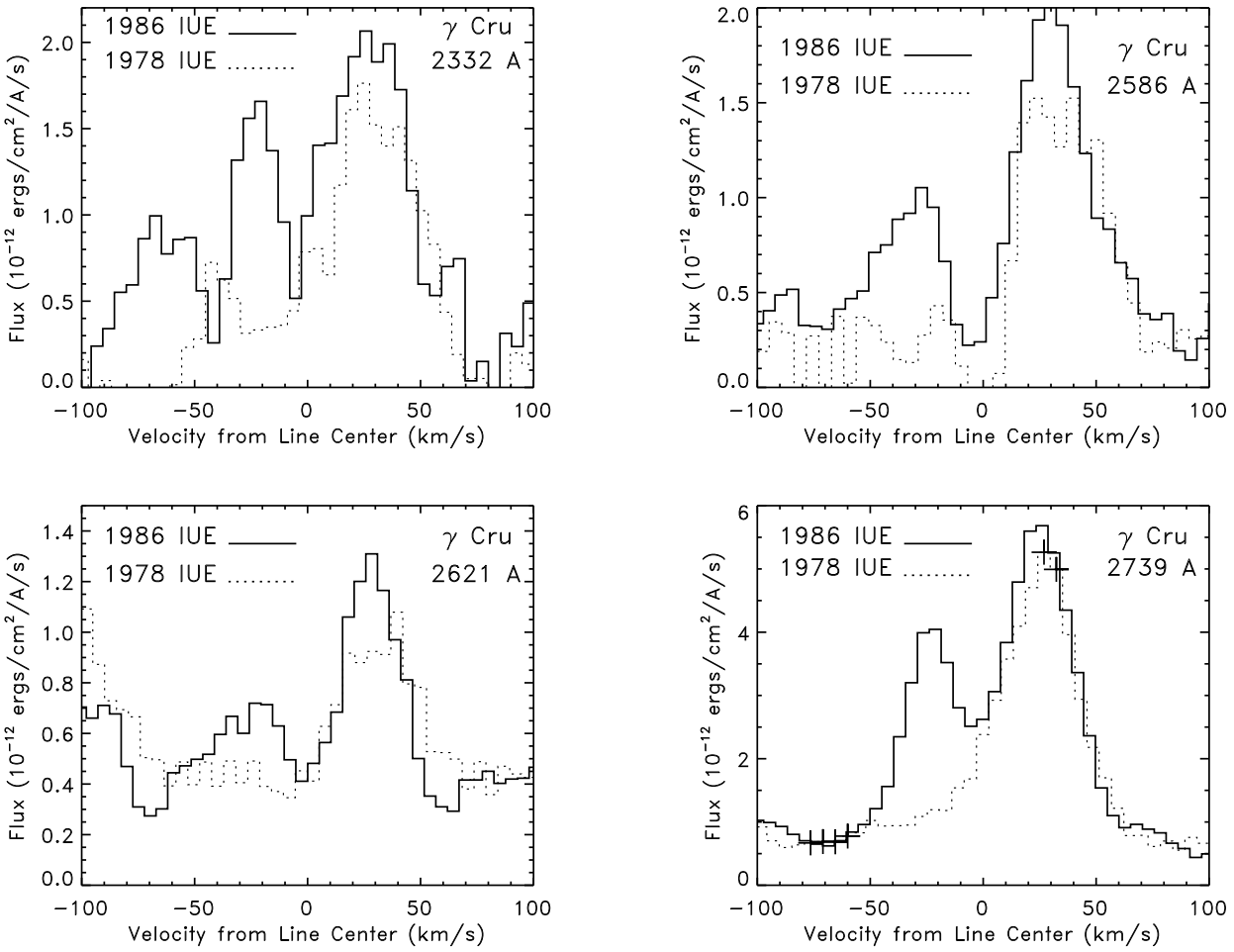


FIG. 2.—Comparison of profiles of four Fe II lines at two epochs in γ Cru. Crosses indicate points of poor quality in *IUE* data (i.e., those affected by saturation of detector pixels or reseau marks on the detector faceplate).

LWP camera is about 1.4 times better than in an equivalent LWR exposure (Barylak 1983), and that fluxes obtained for the same star in exposures obtained by the two cameras may differ from each other by 3%–4% on average (Cassatella et al. 1988). Thus, if we were discussing alterations between two line profiles that were rather subtle (say, at the level of 10% or so), then we would have to view with caution changes between the LWR and LWP images. However, the alterations that appear in Figure 2 are not at all subtle: those alterations in the flux profiles are as large as a factor of 4 at certain wavelengths. Moreover, analogous major changes are seen in the profiles of a large number of lines, over a broad range of locations on the two camera photocathodes (spanning a wavelength range of more than 400 Å in Fig. 2), and these major changes are always seen only on the blue wing of the line. These points lead us to the conclusion that, despite the real differences that exist between LWR and LWP, the alterations between the line profiles of γ Cru at the two epochs shown in Figure 2 are highly significant.

4. OPTICAL THICKNESS IN THE WIND OF λ Vel

Photons associated with a chromospheric emission line are generated in the dense regions of the low to middle chromosphere. An outwardly moving stellar wind will then generate an asymmetry by preferentially scattering photons from the blue side of the line. To investigate this effect we assume that, in the absence of the wind, the intensity on the blue side of the line at a given (negative) velocity $F_b(v)$ would equal the intensity on the red side at the identical (positive) velocity $F_r(v)$. We therefore define an empirical optical depth for the wind at each velocity $\tau_{\rm emp}(v)$ such that $F_b(v)/F_r(v) = e^{-\tau_{\rm emp}(v)}$.

We note that the quantity $\tau_{\rm emp}$ is not necessarily identical to the physical optical depth $\tau_{\rm phys}$ in the wind. Scattering of photons in the blue wing by the wind contributes in certain circumstances to excess photons on the red wing, in which case the photons that contribute to $F_r(v)$ would not arise solely in the chromosphere. The detailed relationship between $\tau_{\rm phys}$ and $\tau_{\rm emp}$ may be quite complicated. For example, complications of a geometrical nature arise from the fact that the disappearance of a blue photon occurs in a *cylinder* along the line to the star, whereas the appearance of a red photon occurs in an *occulted spherical shell*. In one limiting case, where a dense wind has a density scale height $l_\rho \ll R_*$, the blueward absorption trough may be strong, while the redward emission (from a narrow annulus around the disk) may be weak. In the opposite limit, the last scattering may occur so far from the star that the stellar disk subtends only a small solid angle at the radius of the last scattering: in this case the blueward absorption would be weak. Complications of an atomic nature enter into the relationship between $\tau_{\rm emp}$ and $\tau_{\rm phys}$, because there is complex linking between many multiplets of Fe II: these

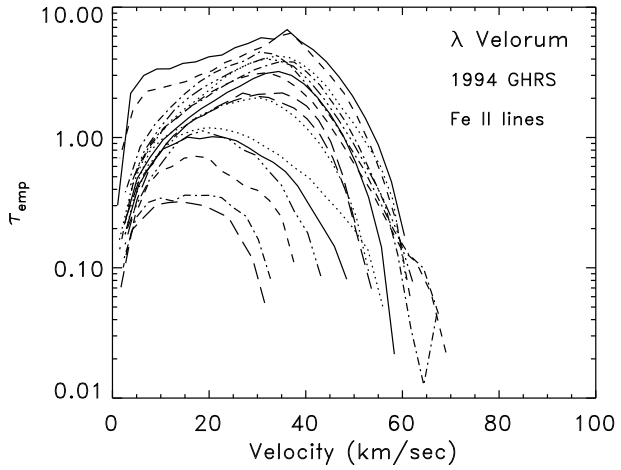


FIG. 3.—Fe II lines formed in the wind of λ Vel in 1994: empirical optical depth τ_{emp} vs. (negative) velocity extracted from the lines listed in Table 2.

linkings modify the line shape and emergent flux. In view of these complications, the process of transforming in detail from τ_{emp} to τ_{phys} is beyond the scope of the present paper. Our aim here is to use a purely empirical measure τ_{emp} to quantify the variations that occur in the wind and then to use a simple model to extract some zeroth-order quantities.

In order to calculate $\tau_{emp}(v)$ for any line, we reflect the line profile about line center after adjusting the wavelength scale to account for the radial velocity of the star. For λ Vel this is $+18$ km s^{-1}. (This effectively assumes that the wings of each line are formed in a medium that is at rest relative to the photosphere.) If a blend occurs at a certain part of the line profile, or if the noise in the line profile becomes comparable to the signal, the τ_{emp} values may fluctuate (spuriously) between positive and negative values. Since we are interested in wind absorption, we consider only positive τ_{emp} values as physically relevant.

In Figure 3 we present $\tau_{emp}(v)$ curves derived from 17 unblended Fe II lines in the GHRS spectra of λ Vel. Details for these lines are presented in Table 2, where the first column lists the laboratory wavelength. The lines that are used in obtaining the τ_{emp} values in Figure 3 span a range of strengths. As a measure of relative line strength, column 2 in Table 2 lists an optical depth parameter τ_0 that has been estimated by Judge (see Carpenter & Robinson 1997). The τ_0 values were calculated assuming line formation in NLTE in a medium of fixed temperature, electron density, and hydrogen column density characteristic of cool star *chromospheres*. These values are used solely to provide an ordering (independent of our τ_{emp} estimates) in terms of relative line strength of the features included in Table 2. The lines in Figure 3 have τ_0 values ranging from 83 to 13899, i.e., an opacity range of more than 100 under chromospheric conditions. In Table 2 we list the maximum value of τ_{emp} for each line and the velocity at which this maximum occurs. The maxima in τ_{emp} range from about 0.3 to almost 10, suggesting that the opacities in the *wind* span a range of about 30, with individual values some 2–3 orders of magnitude smaller than the "chromospheric" values τ_0. The decreases in τ_{emp} relative to τ_0 are caused by decreases of comparable magnitude in electron densities in the wind relative to the chromosphere.

TABLE 2

FE II LINES USED FOR τ_{emp}

λ_{lab} (Å)	τ_0	τ_{emp}(max)	v_{emp}(max) (km s^{-1})
2599.395.....	13899	6.73	36
2598.369.....	4544	4.22	34
2585.876.....	3952	6.32	37
2607.088.....	3537	3.84	35
2332.800.....	2733	4.03	31
2755.737.....	2172	2.20	35
2625.668.....	1754	3.21	34
2739.548.....	1738	2.02	30
2338.001.....	1563	3.15	32
2331.307.....	614	4.53	30
2621.669.....	499	2.19	27
2727.539.....	325	1.01	21
2591.543.....	228	1.12	19
2354.889.....	214	1.19	20
2736.968.....	200	0.72	17
2730.734.....	132	0.36	15
2761.813.....	83	0.32	14

The results shown in Figure 3 and Table 2 exhibit a systematic behavior as we consider lines of increasing opacity. The weakest Fe II lines (those with peak $\tau_{emp} \sim 0.3$) are formed in material with velocities less than 20 km s^{-1}, while stronger lines (those with peak $\tau_{emp} \geq 1$) are formed in faster material. For the strongest lines τ_{emp} peaks at velocities of 35–40 km s^{-1} and then decreases rapidly for $v \geq 40$ km s^{-1} (note the logarithmic scale in the plot). By the time we reach velocities as large as ~ 60 km s^{-1}, all 17 of the Fe II lines have fallen to zero (or negative) values of τ_{emp}. At higher velocities, blends and/or noise prevent us from estimating meaningful values of τ_{emp}.

We have performed preliminary modeling of the line profiles in Figure 3, assuming a spherically symmetric wind and conservative scattering. The results suggest that in 1994 the wind of λ Vel had a terminal velocity v_∞ of about 40 km s^{-1} and a turbulent velocity of 10–15 km s^{-1}.

5. TEMPORAL VARIATIONS IN THE WIND

Values of τ_{emp} have been obtained for many Fe II lines at all of the epochs for which unsaturated UV spectra of λ Vel exist. For any given line, the τ_{emp} values allow us to follow temporal variations in the wind at the locations where that line is formed. An example of the results obtained for one Fe II line is presented in Figure 4. The left panel of Figure 4 shows the τ_{emp} derived from the 1994 GHRS observations, as well as the τ_{emp} derived from *IUE* spectra taken in 1978 and 1982. In all three cases τ_{emp} falls to small values (≤ 0.1) at $v \approx 40$ km s^{-1}.

However, in 1990 (Fig. 4, *right*) τ_{emp} does not fall to small values (≤ 0.1) until v reaches ~ 80 km s^{-1}. In 1990 the peak amplitude of τ_{emp} is also 1.5–2 times larger and the total optical depth (i.e., the area under the τ_{emp} curve) 2–6 times larger than at the other epochs. How robust are the 1990 values of τ_{emp}? To answer this, we created a series of synthetic profiles by adding random noise to each velocity bin of the observed line profile and then recalculating τ_{emp}. The amplitude of the noise is 2 σ, where σ is the standard deviation in the continuum flux near the line in the *IUE* image. The results for seven trial profiles are plotted using plus signs in Figure 4. It can be seen that the differences between 1990 and the other years are statistically highly significant. These results were confirmed through the analysis of a wide variety of lines, including those of Mn II as well as Fe II.

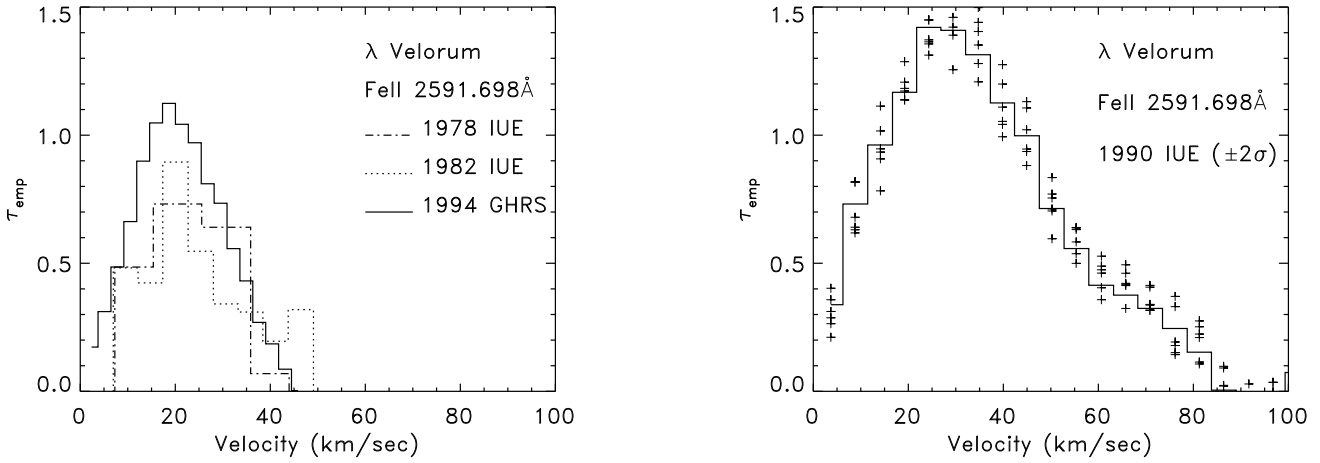


FIG. 4.—Comparison of empirical optical depth τ_{emp} of one Fe II line at four epochs in λ Vel. *Left:* Epochs of slow wind. *Right:* Epoch of fast wind. Crosses in right panel denote values of τ_{emp} when continuum noise is added randomly to each pixel of the line profile.

Preliminary modeling suggests that in 1990, the wind of λ Vel had a terminal velocity v_∞ of 60–70 km s^{-1} and a turbulent velocity of 15–20 km s^{-1}.

We conclude that in 1990 the wind of λ Vel was faster and optically thicker than at the other epochs.

6. DISCUSSION

The aim of this paper is to use a large sample of Fe II lines to quantify the variations that occur in the winds from cool evolved stars. Variations in the winds from certain cool stars have previously been identified by several authors using diagnostics that differ from those we use here.

For example, changes in Mg II and Ca II profiles in several semiregular M giants have been reported by Judge et al. (1993). The profile changes are attributed mainly to alterations in the chromosphere of these pulsating stars, rather than to changes in wind properties.

Temporal variations in Ca II H and K line in K giants and G–K supergiants have been described qualitatively by Reimers (1977). Variability in high-speed wind absorption in Mg II profiles of hybrid stars is mentioned by Drake et al. (1984) as part of their definition of the hybrid class. The timescales of the changes in the profiles of Ca II and Mg II lines in hybrid stars have been reported to be hundreds of days (Ayres et al. 1995; Reimers et al. 1996; Brown et al. 1996). These wind-related changes occur mainly in the violet peak of the Ca II and Mg II lines, which is similar to the "blue-side activity" we report here. For example, Brown et al. (1996) provide illustrations of changes in Mg II profiles in two hybrid stars (α Aqr, G2 Ib, and ι Aur, K3 II) that are similar to what we see in the Fe II profiles from the noncoronal stars λ Vel and γ Cru. The most quantitative description of the changes in the winds of hybrid stars appears in Brown et al. (1996), who note a change of 25 km s^{-1} in the terminal velocity of the wind from the G2 Ib hybrid star α Aqr in a 6 month interval. We note that the Mg II and Ca II resonance lines (which have been used in all of the above studies) are so strong that they probe mainly the variations that occur in the outermost regions of the winds.

In this paper we utilize GHRS and *IUE* data to evaluate quantitatively the variations that occur in the wind from the single noncoronal K star λ Vel. Specifically, we broaden the range of heights (or radial distances) in the wind that are probed by choosing a sample of 17 Fe II lines with a broad range of relative optical depths: the optical depth in our strongest line is more than 100 times greater than in our weakest line. Using this sample of Fe II lines, we find that the wind varies in terminal velocity by at least 20 km s^{-1} and in total optical depth by factors of 2–6 on timescales of several yr. The total optical depth of the wind is largest at the epoch when the wind is fastest. These variations in wind properties lead to dramatic alterations on the blue side of the Fe II profiles of lines formed in the wind: the alterations are such that the blue "peak" of certain lines may disappear altogether at certain epochs. Equally dramatic alterations on the blue side of Fe II line profiles have also been found in the wind of the single noncoronal M type giant γ Cru on similar timescales (Carpenter 1986, 1987), as shown in Figure 2.

The profiles of the Fe II lines are well suited to the study of wind variations of our target stars, since their widths (in velocity space) are comparable to the wind speed. In contrast, the Ca II and Mg II profiles are much broader (in velocity space) than the winds that we study here. The Ca II and Mg II profiles are therefore better suited for probing stars like the hybrids Mullan (1984), where the winds are faster than those we consider here.

Brown et al. (1996) ascribe wind-related profile changes to variations in wind opacity (caused by rotation of a high-opacity structure out of the line of sight or to its dissolution) or to variations in the wind acceleration rate. Here we speculate that coronal mass ejections may be an alternative explanation. There is spectroscopic evidence suggesting that CMEs are present in the wind from a high-gravity K star (Mullan et al. 1989). If new magnetic flux emerges at the surface of λ Vel or γ Cru, the low gravity in these two stars facilitates the opening up of the magnetic fields by thermal pressure (Mullan & Steinolfson 1983). Thus, conditions are favorable in these stars for the creation of CMEs. We speculate that we might have "caught" a CME ejection that emerged close to our line of sight in 1990 (λ Vel) and in 1978 (γ Cru).

The work of D. J. M. has been supported by the NASA/ASEE Summer Faculty Fellowship Program and the NASA Space Grant College program. Additional support has been provided by NASA through an STScI grant for GO program 5307.

REFERENCES

Ayres, T. R., et al. 1981, ApJ, 250, 293
———. 1995, ApJS, 96, 223
Barylak, M. 1983, *IUE* Newsl. 21
Brosius, J. W., & Mullan, D. J. 1986, ApJ, 301, 650
Brown, A., Deeney, B. D., Ayres, T. R., Veale, A., & Bennett, P. D. 1996, ApJS, 107, 263
Carpenter, K. G. 1986, in New Insights in Astrophysics, ed. E. J. Rolfe (Noorwijk, Netherlands: ESA SP-263,), 99
Carpenter, K. G. 1987, in Physics of Formation of Fe II Lines Outside LTE, ed. R. Viotti, A. Vittone, & M. Friedjung (Dordrecht: Reidel), 95
Carpenter, K. G., & Robinson, R. D. 1997, ApJ, 479, 970
Cassatella, A., Lloyd, C., & Gonzalez Riestra, R. 1988, *IUE* Newsl. 35, 225
Drake, S. A., Brown, A., & Linsky, J. L., ApJ, 284, 774
Hartmann, L., Dupree, A., & Raymond, J. 1980, ApJ, 236, L143
Jackson, B. V., & Howard, R. A. 1993, Sol. Phys., 148, 359
Judge, P. G., Luttermoser, D. G., Neff, D. H., Cuntz, M., & Stencel, R. E. 1993, AJ, 105, 1973
Leer, E., Holzer, T., & Fla, T. 1982, Space Sci. Rev., 33, 161
Mullan, D. J. 1984, ApJ, 284, 769
Mullan, D. J., et al. 1989, ApJ, 339, L33
Mullan, D. J., & Steinolfson, R. S. 1983, ApJ, 266, 823
Reimers, D. 1977, A&A, 57, 395
Reimers, D., et al. 1996, A&A, 310, 813